ANTICANCER RESEARCH *38*: 5693-5701 (2018)
doi:10.21873/anticanres.12906

miR-3148 Is a Novel Onco-microRNA that Potentiates Tumor Growth *In Vivo*

TAKAKI AKAMINE[1,2], YOSUKE MORODOMI[1,2], YUI HARADA[2], KOJI TERAISHI[1,2], TETSUZO TAGAWA[1], TATSURO OKAMOTO[1], YOSHIHIKO MAEHARA[1] and YOSHIKAZU YONEMITSU[2]

[1]*Department of Surgery and Science, Graduate School of Medical Sciences, Kyushu University, Fukuoka, Japan;*
[2]*R&D Laboratory for Innovative Biotherapeutics, Graduate School of Pharmaceutical Sciences, Kyushu University, Fukuoka, Japan*

Abstract. *Background/Aim: Alterations of microRNA expression in three-dimensional spheroids were examined to identify novel microRNAs that might be associated with tumorigenesis. Materials and Methods: Using microRNA microarray analysis, we screened for microRNAs that were dramatically up-regulated inside three-dimensional spheroids in genetically-modified HCT116 human colon cancer cells expressing Copepoda Green Fluorescent Protein under hypoxia. Results: miR-3148 was identified as a possible candidate onco-microRNA. A growth advantage of HCT116 cells stably expressing miR-3148 (HCT116-miR3148) was observed compared to parental cells in vivo, but not in vitro. Additionally, no change in growth under hypoxic or starvation conditions was seen in these cells cultured two-dimensionally; however, HCT116-miR3148 cells maintained as three-dimensional spheroids were highly resistant to hypoxic conditions. HCT116-miR3148 cells were more sensitive to mitogen-activated protein kinase (MAPK) kinase inhibitors and extracellular signal-regulated kinase (ERK) inhibitors. Conclusion: MiR-3148 may be a novel onco-microRNA that protects cancer cells from serious stress conditions through the MAPK/ERK pathway, especially in vivo.*

MicroRNAs (miRNAs or miRs) are 21-25 nt single-stranded RNA molecules that regulate post-transcriptional gene expression by targeting the 3'-untranslated regions of certain mRNAs (1). During the past decade, miR-mediated gene regulation has attracted increasing attention as a potential mechanism of carcinogenesis, tumor proliferation, differentiation, and invasion (2). miRNAs capable of stimulating carcinogenesis and tumor progression are known as 'onco-miRs', and have often been identified as inhibitors of tumor suppressor genes (3). However, the exact role of these onco-miRs *in vivo*, and particularly in clinical settings, is uncertain.

Three-dimensional (3D) cell cultures, so-called sphere formation assays, mimic *in vivo* conditions more accurately than cells cultured in two-dimensional (2D) monolayers (4, 5). Sphere formation creates different internal and external environments in terms of oxygen, lactate, glucose, or adenosine triphosphate (ATP) concentrations (6). These normoxic, hypoxic, or near necrotic areas potentially reflect the heterogeneity of human solid tumors. It is also now widely accepted that 3D sphere culture systems show stem cell-like functional properties such as self-renewal, drug resistance, and tumorigenicity in xenograft models (7-9). A recent report by Riedl *et al.* indicated that 3D spheroid formation dramatically altered cellular signal transduction pathways including AKT, mammalian target of rapamycin, ribosomal protein S6 kinase, and the mitogen-activated protein kinase (MAPK) pathway, resulting in changes to cellular responses against drug treatments (10). Such studies highlighted the importance of 3D culture systems for understanding cancer biology; however, little is known about the dynamics of onco-miRs during 3D formation.

Therefore, the present study aimed to identify novel onco-miRs that regulate tumor formation in genetically engineered HCT116 human colorectal cancer cells expressing Copepoda Green Fluorescent Protein (copGFP) under hypoxia-responsible elements. A novel candidate, miR-3148, was identified in 3D spheroid culture that regulated tumor growth *in vivo* rather than *in vitro*.

Correspondence to: Yoshikazu Yonemitsu, MD, Ph.D., R&D Laboratory for Innovative Biotherapeutics, Graduate School of Pharmaceutical Sciences, Kyushu University, 6th Floor, Collaborative Research Station I, 3-1-1 Maidashi, Higashi-ku, Fukuoka 812-8582, Japan. Tel: +81 926426337, Fax: +81 926426342, e-mail: yonemitu@med.kyushu-u.ac.jp

Key Words: MicroRNA-3148, onco-miR, spheroid, colon cancer.

Materials and Methods

Cell culture and reagents. The human colon cancer cell line HCT-116 was cultured in RPMI-1640 medium supplemented with 10% fetal bovine serum (FBS), 100 units/ml penicillin, and 100 μg/ml streptomycin. Cells were maintained in a humidified atmosphere of 5% CO_2 in air at 37˚C, and were used at passages 4-10. Nunclon™ Delta-treated dishes (Thermo Fisher Scientific, Rockford, IL, USA) were used for adherent cultures. For sphere formation, cells were cultured in Lipidure®-Coat 96-well plates (Thermo Fisher Scientific). For hypoxia induction, cells were cultured in multigas incubators (SANYO, Osaka, Japan). Nitrogen gas was supplied to the chambers to control the oxygen concentration. Pemetrexed (LKT Laboratories Inc., St. Paul, MN, USA), irinotecan (LKT Laboratories), 5-fluorouracil (5-FU; InvivoGen, San Diego, CA, USA), temsirolimus (Abcam, Cambridge, UK), CH4987655 (Chugai Pharmaceutical, Tokyo, Japan), PD-0325901 (Cayman Chemicals, Ann Arbor, MI, USA), SCH772984 (Selleck Chemicals, Houston, TX, USA), and GDC-0994 (Ravoxertinib; Selleck Chemicals) were used in cell sensitivity assays.

Establishment and characterization of a hypoxia-responsive cell line. Hypoxia-responsive cells were produced using a hypoxia-inducible factor (HIF)-1 reporter system with the pGreenFire lentivirus vector (System Biosciences, Palo Alto, CA, USA). Briefly, the vector contained a HIF-1 reporter construct that expresses copGFP in a hypoxic environment under the control of the mCMV promoter. HCT-116 cells were infected with the lentivirus, then purified and cloned. Cloned cells that were stable in a hypoxic environment (HCT116-HIF1) were used in subsequent investigations.

miR analysis. To identify the status of miRs in the hypoxic region of a spheroid, miR expression profiling was performed using miR microarray technology. After the assembly of a few dozen HCT116-HIF1 spheroids, those were dissociated into single cells with gentle pipetting in medium with FACSmax Cell Dissociation Solution (Genlantis Inc., CA, USA). Cells were sorted by copGFP expression using an SH800 cell sorter (SONY, Japan). Dead cells were excluded by staining with propidium iodide. Data analysis was performed using SH800 software or Flow Jo 19.1 software (Tree Star, Inc., Ashland, OR, USA). Total RNA was extracted using ISOGEN II (NIPPON GENE, Tokyo, Japan), and its concentration was determined with a NanoDrop 2000 spectrophotometer (Thermo Fisher Scientific). RINs were determined using the 2100 Bioanalyzer (Agilent Technologies, Santa Clara, CA, USA) (11). Global miR expression profiles of RNA samples were obtained using a Toray's human miR microarray platform based on miRBase version 19 (3D-Gene miRNA oligo chip, Toray Industries Inc., Tokyo, Japan), as previously described (12). In this study, the median values of the foreground signal minus the local background were calculated as the feature intensities.

Kaplan–Meier plotter analysis. The Kaplan–Meier plotter tool (www.kmplot.com/mirpower), a database that combines miR expression and clinical data of breast cancer, was used to analyse the prognostic value of miRs (13). The Kaplan–Meier survival plot and the hazard ratio with 95% confidence intervals and log-rank *p*-values were calculated in the fitted tool. The Cancer Genome Atlas and METABRIC data sets were used in this analysis.

Establishment of a miR-3148-expressing stable transfectant. To evaluate the functional effects of overexpressing miR-3148 in colon cancer cell lines, the pLV-[hsa-mir-3148] plasmid (Biosettia Inc., CA, USA) expressing miR-3148 was transfected into HCT-116 cells using Lipofectamine 3000 reagent (Thermo Fisher Scientific). Stably transfected clones were isolated using an SH800 cell sorter (SONY, Japan).

Cell proliferation. Cell lines were subcultured every 3 days and the number of cells was determined by manual counting. Days in culture following cell seeding were plotted on the x-axis, and cumulative cell number (log scale) was plotted on the y-axis.

Animal studies. Animal experiments were reviewed and approved by the Institutional Committee for Animal Care and Use of Kyushu University (A26-240-0) and by the Biosafety Committee for Recombinant DNA Experiments of Kyushu University (27-67). The experiments were also performed in accordance with recommendations for the proper care and use of laboratory animals and according to The Law (No. 105) and Notification (No. 6) of the Japanese Government.

Four-week-old male balb/c nu/nu mice (Charles Liver Grade; KBT Oriental, Tosu, Saga, Japan) were kept in humane conditions in the animal care facility. After adequate anesthesia, appropriate numbers of HCT-116 tumor cells in 100 μl Hank's buffered salt solution were injected subcutaneously into the flanks of the mice. The tumor volume was assessed using microcalipers every 3 to 4 days after the inoculation of cells according to the formula: tumor volume (mm^3)=S2×L/2, where L and S indicate the longest and shortest part of the tumor, respectively.

Cell viability and cytotoxicity assays. Cell viability was measured using the CellTiter-Glo™ 2D reagent (Promega, Madison, WI, USA), which is based on the measurement of ATP. Each experiment was performed in triplicate. Briefly, HCT116 cells were seeded at a density of 4.5×10^3 cells per well of Nunclon™ 96-well optical-bottom plates (Thermo Fisher Scientific). After 24 h incubation at 37˚C, dimethyl sulfoxide (DMSO), pemtrexed, iricnotecan, 5-FU, temsilolimus, mitogen-activated protein kinase kinase (MEK) inhibitors (CH4987655 and PD-0325901) and extracellular signal-regulated kinase (ERK) inhibitors (Ravoxertinib and SCH772984) were added, and cells were incubated for an additional 72 h. CellTiter-Glo™ 2D was added to the cell culture, and luminescence was measured using the Glo-Max Discover System (Promega). Cell viability was expressed relative to DMSO-treated controls.

3D spheroid viability was measured using the CellTiter-Glo® 3D reagent (Promega). Briefly, HCT116 cells were seeded at a density of 1×10^3 cells per well of 96-well low-attachment EZ-BindShut plates (IWAKI, Chiba, Japan). CellTiter-Glo® 3D reagent was added to each well daily, and the luminescence signal generated by ATP was read after 30 min with the Glo-Max Discover System and expressed as relative luminescence units (RLUs). Days in culture following cell seeding were plotted on the x-axis, and RLU was plotted on the y-axis.

Statistical analyses. All data were expressed as means±standard deviations. Data were compared using one-way ANOVA and the Student's *t*-test. Survival curves were determined using the Kaplan–Meier method, and the log-rank test was used for comparison. A probability value of $p<0.05$ was considered statistically significant. All analyses were performed using JMP 11.0.0 software (SAS Institute Inc., Cary, NC, USA).

Table I. *Up-regulated miRs inside HCT116 spheroids and in silico analysis based on the Kaplan–Meier plotter.*

miR	Signal strength		Out/in ratio	*p-Value	HR (95%CI)	KM plotter symbol list
	Inside/GFP+	Outside/GFP–				
hsa-miR-3148	113	0	–	6.9E10-7	4.05 (2.23–7.35)	hsa-miR-3148
hsa-miR-3184-5p	103.5	11.4	0.11	6.0E10-7	4.07 (2.24–7.39)	hsa-miR-3184
hsa-miR-1273a	71.7	10.7	0.15	–	–	–
hsa-miR-335-5p	29.6	8	0.27	3.91E-02	2.01 (1.02–3.94)	hsa-miR-335
hsa-miR-6510-5p	24.3	8.1	0.33	–	–	–
hsa-miR-210	636.6	214.8	0.34	7.1E10-4	2.86 (1.52–5.41)	hsa-miR-210
hsa-miR-2113	34.8	11.9	0.34	1.1E10-6	3.96 (2.18–7.19)	hsa-miR-2113
hsa-miR-1185-1-3p	26.8	9.2	0.34	1.0E10-1	0.66 (0.40–1.09)	hsa-miR-1185
hsa-miR-138-1-3p	28	9.6	0.34	1.4E10-2	0.67 (0.39–1.14)	hsa-miR-138
hsa-miR-4725-5p	25.2	8.7	0.34	–	–	–
hsa-miR-1273e	125.3	44.7	0.36	–	–	–
hsa-miR-17-3p	46.9	16.9	0.36	3.6E10-2	1.72 (1.03–2.88)	hsa-miR-17
hsa-miR-939-3p	22.2	8.1	0.36	2.5E10-2	1.35 (0.81–2.27)	hsa-miR-939
hsa-miR-34a-5p	149.6	54.6	0.37	7.6E10-2	1.57 (0.95–2.61)	hsa-miR-34a
hsa-miR-145-5p	70.7	25.9	0.37	4.7E10-2	1.74 (1.00–3.01)	hsa-miR-145
hsa-miR-4739	906.1	332.7	0.37	–	–	–
hsa-miR-4487	23	8.5	0.37	–	–	–
hsa-miR-575	325.5	121.1	0.37	2.1E10-2	1.31 (1.04–1.64)	**hsa-miR-575

*Log-rank p-Value and the hazard ratio with 95% confidence intervals were obtained using the symbol in the KM plotter analysis at http://kmplot.com/analysis/. **Survival analysis was performed by array based on the METABRIC data set. HR: Hazard ratio; CI: confidence interval; KM plotter: Kaplan–Meier plotter.

Results

Identification of miR-3148 as an up-regulated miR inside HCT116 3D spheroids. To identify novel onco-miRs that are up-regulated inside spheroids, we focused on the internal spheroid environment that mimics a hypoxic lesion (6). We established the cell line HCT116-HIF1 which expresses copGFP under hypoxia-responsible elements that are HIF-1 binding sites. Figure 1A shows the microscopic findings of HCT116-HIF1 cells in 2D and 3D cultures. copGFP expression was observed in 2D culture under hypoxia (1% O_2) and in 3D culture inside spheroids.

HCT116-HIF1 spheroids were then dissociated into single cells using FACSmax, and the cells were separated into those inside (copGFP-positive) and outside (copGFP-negative) 3D spheroids according to copGFP expression levels using a cell sorter (Figure 1B). Total RNA extracted from sorted cells was of an acceptable quality, with RNA integrity numbers (RINs) of 9.3 inside and 10 outside. Findings of miR microarray analysis comparing miR expression inside and outside the spheroids are shown in Figure 1C as a scatter plot, and a list of the top 20 most significantly elevated miRs inside the spheroid compared with outside is shown in Table I. Analysis of the prognostic value of each miR by online *in silico* Kaplan–Meier plotter analysis showed that miR-3148 was most strongly related to the overall survival of breast cancer patients. Since survival data of colon cancer patients were not available, Kaplan–Meier plotter analysis was performed in breast cancer patients. We therefore focused on the function of miR-3148 (Table I, Figure 1D). miR-3148 was not represented as a plot in Figure 1C because its expression outside the spheroids was below measurable limits.

miR-3148 has tumorigenic potential in vivo but not in vitro. To identify the biological function of miR-3148, HCT116 cells stably expressing miR-3148 (HCT116-miR3148) were established. Parental HCT116 cells were hereafter known as HCT116-P cells. As shown in Figure 2A, miR-3148 expression had no effect on the proliferation of HCT116 cells *in vitro*. On the other hand, *in vivo* tumor growth in male nude mice was significantly more pronounced from HCT116-miR3148 cells than with HCT116-P cells ($p<0.05$; Figure 2B and C).

miR-3148 promoted resistance to hypoxic conditions in 3D culture but did not affect growth under hypoxia or nutrient starvation in 2D culture. We next investigated the proliferation of HCT116-miR3148 cells under hypoxia (1% O_2) and nutrient-starved conditions (FBS 1%) which were similar to the internal environment of the spheroid. However, no difference was observed between the proliferation of HCT116-P and HCT116-miR3148 cells

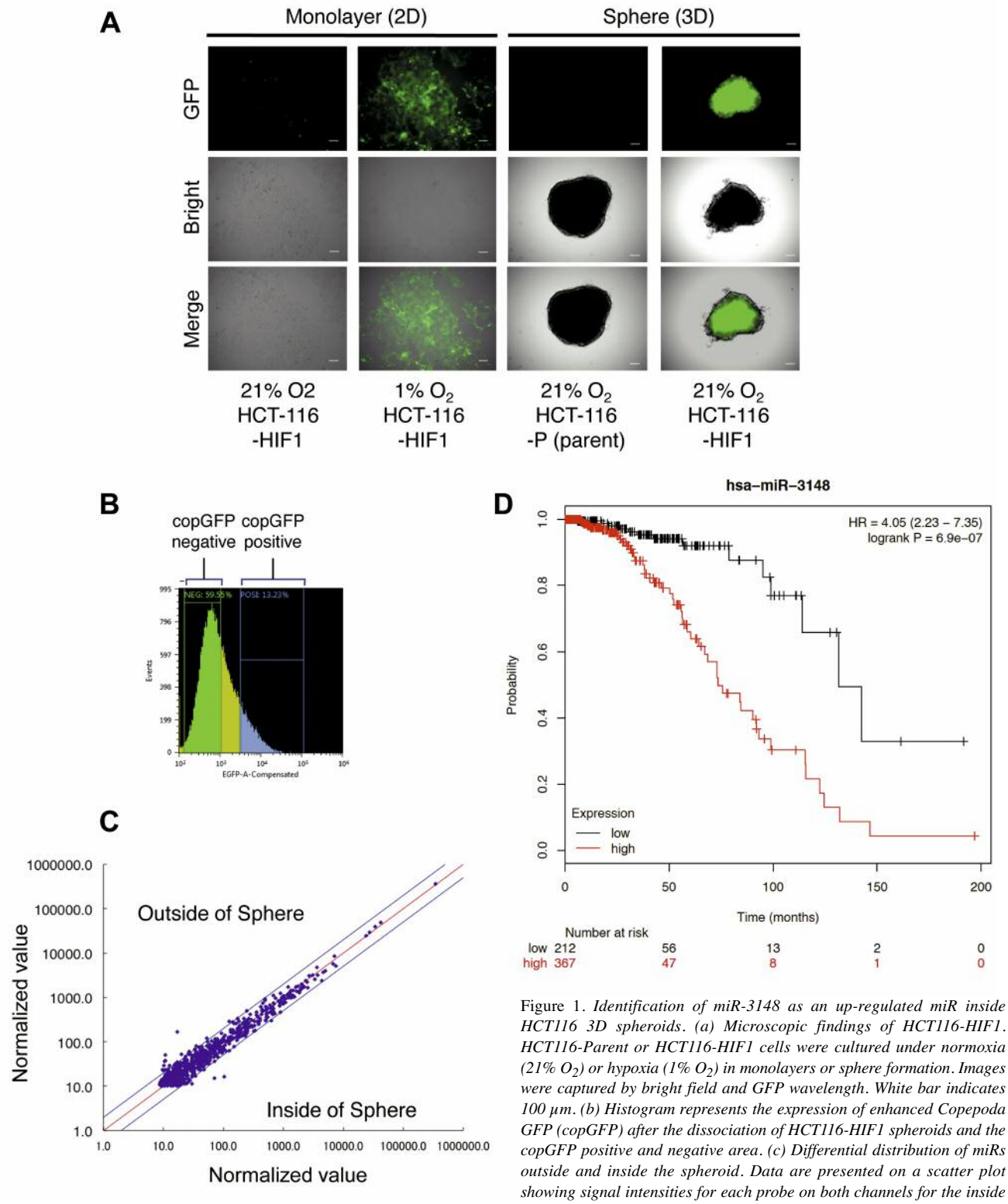

Figure 1. *Identification of miR-3148 as an up-regulated miR inside HCT116 3D spheroids. (a) Microscopic findings of HCT116-HIF1. HCT116-Parent or HCT116-HIF1 cells were cultured under normoxia (21% O_2) or hypoxia (1% O_2) in monolayers or sphere formation. Images were captured by bright field and GFP wavelength. White bar indicates 100 μm. (b) Histogram represents the expression of enhanced Copepoda GFP (copGFP) after the dissociation of HCT116-HIF1 spheroids and the copGFP positive and negative area. (c) Differential distribution of miRs outside and inside the spheroid. Data are presented on a scatter plot showing signal intensities for each probe on both channels for the inside and outside of the spheroid. The x-axis is the normalized value of the gene expressed inside the spheroid and the y-axis is outside the spheroid. The region between the two blue lines represents up to a 2-fold change in miR expression. (d) Kaplan–Meier plotter analysis showing that miR-3148 was an unfavorable prognosis factor (p<0.001).*

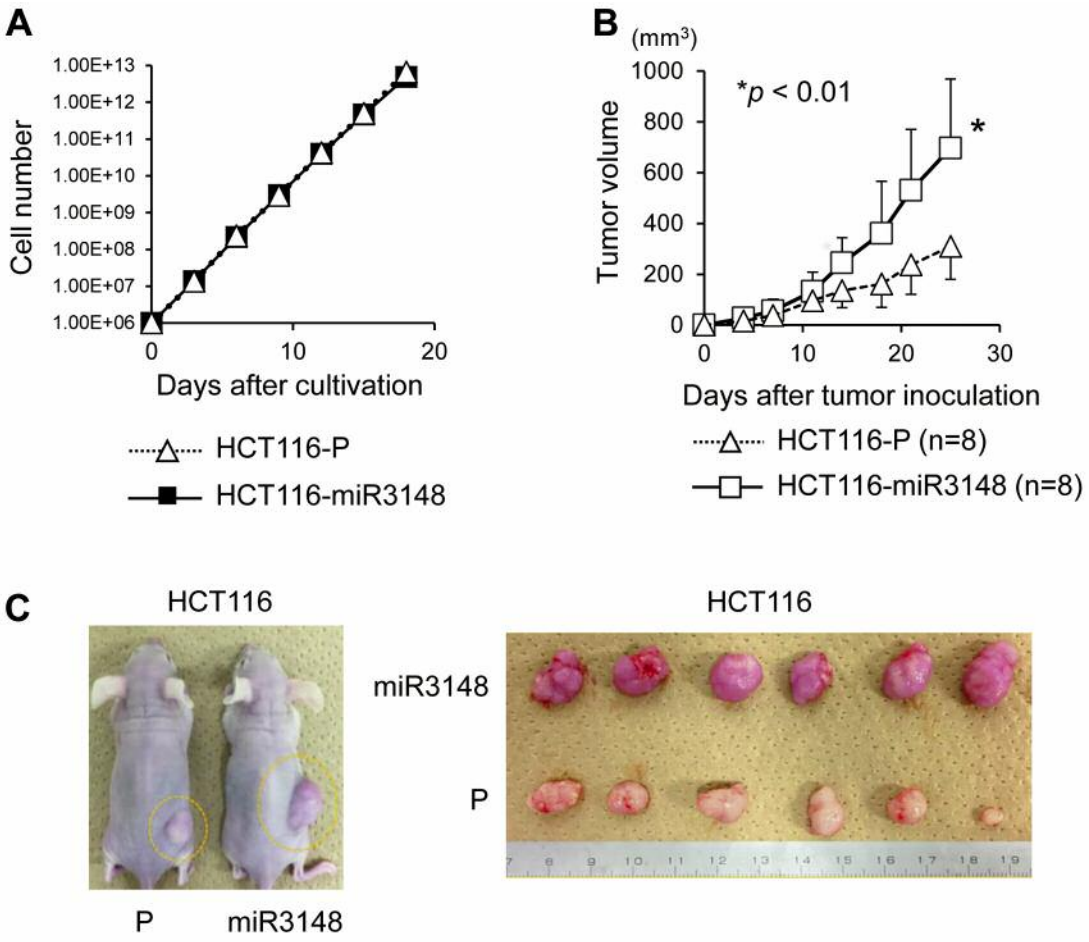

Figure 2. *miR-3148 expression is involved in tumor progression in vivo but not in vitro. (a) Cell proliferation assay of HCT116-miR3148 and HCT116-Parent cells. (b) Subcutaneous tumor growth curves for HCT116-miR3148 (n=8) and HCT116-Parent (n=8) cells in vivo. (c) Macroscopic findings of xenograft mice carrying HCT116-miR3148 tumors (right) and HCT116-Parent tumors (left). Error bars indicate standard deviations.*

(Figure 3A). Assessment of cell viability under normoxia and hypoxia showed that HCT116-miR3148 spheroids were highly resistant to hypoxic conditions compared with HCT116-P spheroids (Figure 3B). These results suggested that miR-3148 reacted to severe stress in 3D, but not in 2D culture.

miR-3148 expression induced sensitivity to MEK inhibitors and ERK inhibitors in HCT116 cells. To investigate additional characteristics of miR-3148, HCT116-miR3148 cell sensitivity to anticancer agents such as pemetrexed (an antifolate agent), irinotecan (a DNA topoisomerase-I inhibitor), 5-FU (an antimetabolite agent), temsirolimus (a mammalian target of rapamycin inhibitor), MEK inhibitors, and ERK inhibitors were evaluated. HCT116-miR3148 cells were shown to be more sensitive to both MEK and ERK inhibitors than HCT116-P cells (Figure 4A and B).

Discussion

In the present study, changes in miR expression in the core of spheroids were investigated in order to identify novel onco-miRs. Our major findings were: (i) the remarkable up-regulation of miR-3148 expression inside HCT116 spheroids; (ii) a growth advantage of HCT116-miR3148 cells compared to HCT116-P cells *in vivo,* but not *in vitro*, even under stress conditions such as hypoxia and starvation; (iii) the high resistance of HCT116-miR3148 cells maintained as 3D spheroids to hypoxic conditions; and (iv) the increased sensitivity of HCT116-miR3148 cells to both MEK and ERK inhibitors compared with HCT116-P cells. These findings suggest that miR-3148 may be a novel onco-miR that protects cancer cells from serious stress conditions through the MAPK/ERK pathway, especially *in vivo*. This is the first study to report changes of miR expression in 3D spheroids.

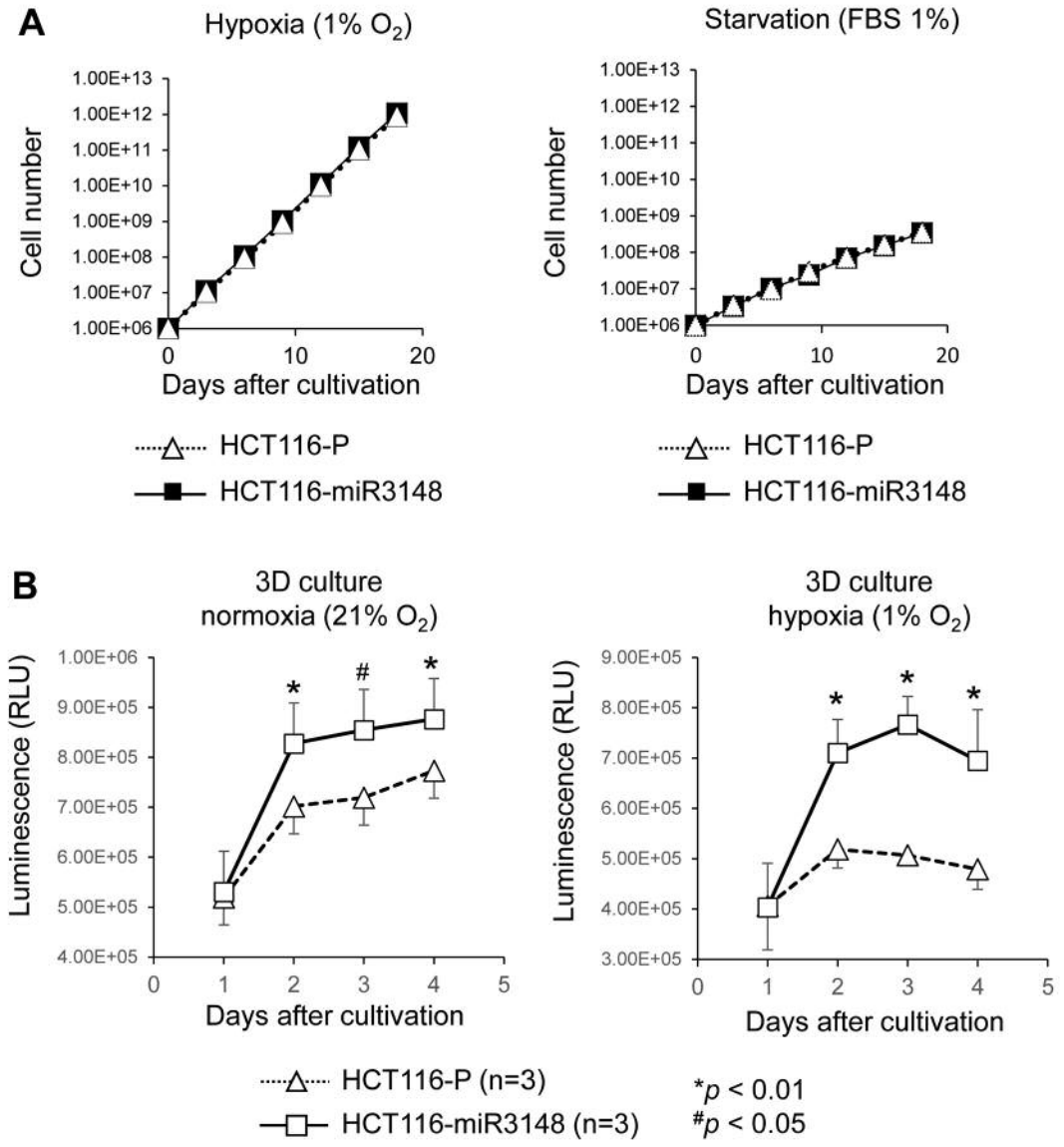

Figure 3. *mir-3148 promotes resistance to hypoxic conditions in 3D but does not affect growth under hypoxia or nutrient starvation in 2D culture. (a) Cell proliferation assay of HCT116-miR3148 and HCT116-Parent cells under hypoxia and serum starvation. (b) Cell viability assay of spheroids under normoxia (21% O_2) and hypoxia (1% O_2).*

The observed increase in miR-3148 expression within the spheroids and its association with unfavorable prognosis in Kaplan–Meier plotter analysis (Figure 1D and Table I) suggested that it could function as an onco-miR.

miR-3148 is located on Chromosome 8, NC_000008.11, and has no surrounding signature genes. However, the observed up-regulation could be explained as induction by a stress factor. Indeed, our microarray analysis showed that miR-210, miR-145, and miR34a were all up-regulated inside spheroids (Table I) under conditions of hypoxia or serum starvation (14-16).

We speculate that miR-3148 has dual roles as an onco-miR. The first is its contribution to an environment that benefits the survival of cancer cells under conditions of stress. In support of this, HCT116-miR3148 cells maintained as 3D spheroids were highly resistant to hypoxic conditions (Figure 3B). Sphere formation might have important implications in clinical or pathological settings. For example, some types of cancer such as ovarian or breast cancer tend to form cell clusters, which resemble sphere formation in dissemination of the pleural and peritoneal cavity, and may contribute to tumor progression (17). Moreover, we recently

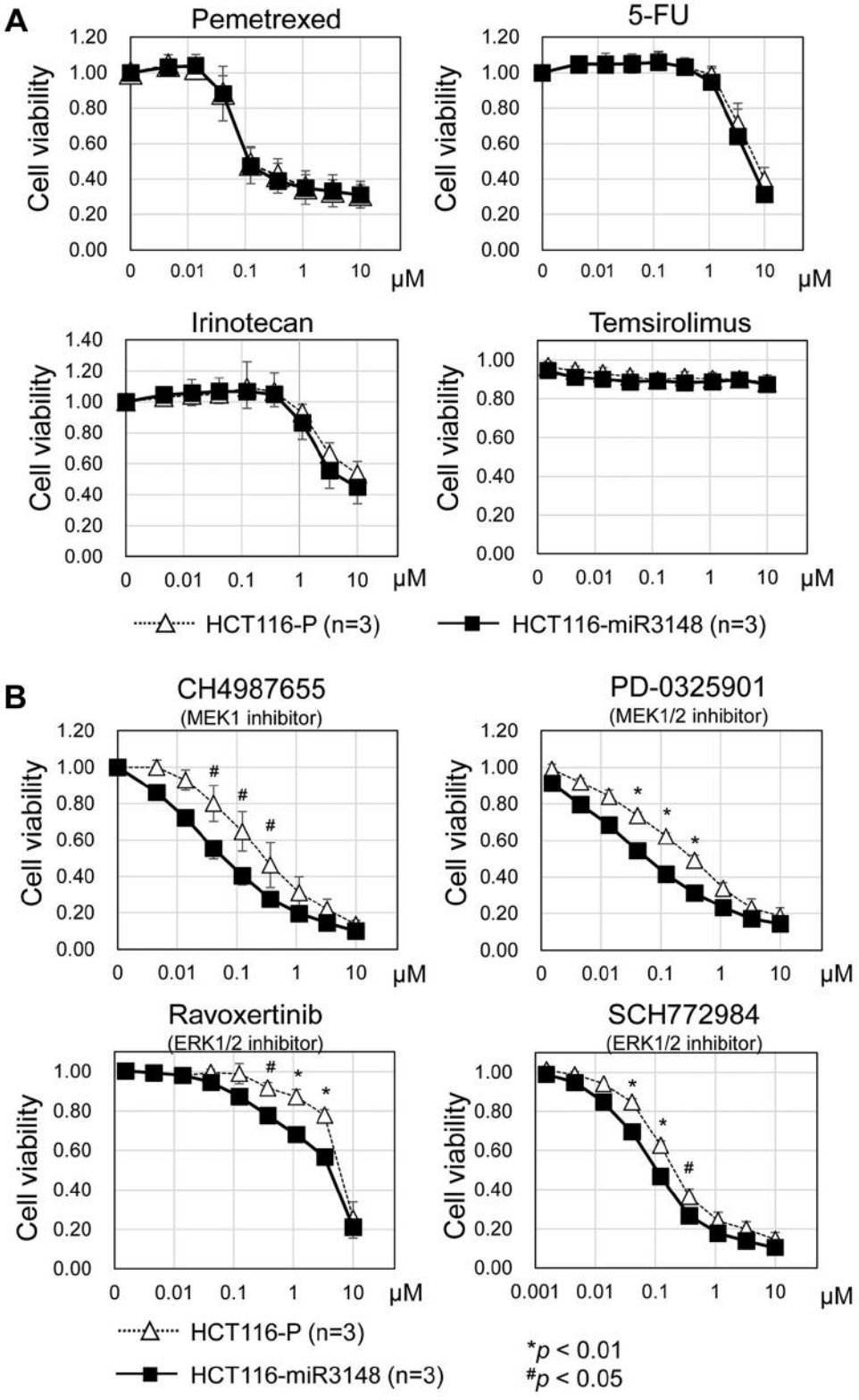

Figure 4. *HCT116-miR3148 cells are more sensitive to MEK and ERK inhibitors than HCT116-Parent cells. (a) HCT116-Parent and HCT116-miR3148 cells were treated with pemetrexed, irinotecan, 5-fluorouracil and temsirolimus; and (b) MEK inhibitors (CH4987655 and PD-0325901) and ERK inhibitors (Ravoxertinib and SCH772984). Relative cell viability (%) was expressed as a percentage relative to untreated control cells. Data are expressed as means±standard deviations based on three independent experiments.*

reported that Sp1-mediated overexpression of CXCR4 induced by sphere formation played an essential role in directional metastasis during tumor dissemination in the peritoneum (18).

The second role is that tumor-derived miR could act as an immunosuppressor in the tumor microenvironment. Recently, tumor-derived exosomal miR has been shown to contribute to tumor-mediated immunosuppression (19, 20). Additionally, in a previous report, Deng *et al*. demonstrated that miR-3148 suppressed toll-like receptor 7 (TLR7), which functions in immunity, and that the TLR7 agonist imiquimod was efficacious in the immunotherapy of skin cancer and cutaneous metastasis (21, 22). It is possible that exosomal miRs derived from the cancer microenvironment influence dendritic cells to suppress TLR7, leading to the inhibition of cancer immunity. In other words, the cell microenvironment itself could be a cause of tumor progression, which explains our observed tumor growth *in vivo* but not *in vitro* (Figure 2B-D).

miR-3148 was also previously shown to be associated with chronic thromboembolic pulmonary hypertension, and *in silico* analysis suggested that it was involved in the protein kinase C alpha (PRKCA) cancer pathway (23). More recently, loss of PRKCA-induced colony growth in 3D matrigel culture and tumor growth *in vivo* were reported in Kras-mutant lung cancer cells (24). Because MAPK/ERK signaling lies downstream of mutant Kras, these previous reports support our finding that HCT116-miR3148 cells were more sensitive to MEK and ERK inhibitors than HCT116-P cells.

Limitations of our study were that although miR expression changes were detected within spheroids, the precise mechanisms of these changes were not fully investigated, nor miR-3148 target genes were examined. Moreover, the universality of this phenomenon is yet to be determined because only one cell line was assessed. Additionally, this study focused exclusively on miR-3148, but other miRs warrant investigation because they may function synergistically within tumors. From our data, we envision a novel therapeutic approach for solid tumors in which the prevention of cancer cell condensation might stop the formation of hypoxic lesions and the acquisition of malignant properties.

In summary, a dramatic up-regulation of miR-3148 expression inside spheroids was identified, suggesting that it might be a novel onco-miR that protects cancer cells from serious stress conditions through the MAPK/ERK pathway, especially *in vivo*. These findings suggest that the prevention of tumor cell condensation might be a novel therapeutic strategy.

Conflicts of Interest

The Authors declare no conflict of interest.

Acknowledgements

The Authors thank Naomi Ono, Risa Tanaka, Ryoko Nakamura, and Natsumi Maeda (R&D Laboratory for Innovative bioTherapeutics Science) for technical assistance. The Authors also acknowledge the gift of CH4987655 from Chugai Pharmaceutical Co. The Authors also thank Sarah Williams, PhD, from Edanz Group (www.edanzediting.com) for editing a draft of this manuscript. This work was supported by MEXT KAKENHI (Grant Number 15H05792) and the KAIBARA MORIKAZU MEDICAL SCIENCE PROMOTION FOUNDATION.

References

1 He L and Hannon GJ: MicroRNAs: small RNAs with a big role in gene regulation. Nat Rev Genet *5*: 522-531, 2004.
2 Lin S and Gregory RI: MicroRNA biogenesis pathways in cancer. Nat Rev Cancer *15*: 321-333, 2015.
3 Taylor MA and Schiemann WP: Therapeutic opportunities for targeting microRNAs in cancer. Mol Cell Ther *2*: 1-13, 2014.
4 Dolznig H, Rupp C, Puri C, Haslinger C, Schweifer N, Wieser E, Kerjaschki D and Garin-Chesa P: Modeling colon adenocarcinomas *in vitro* a 3D co-culture system induces cancer-relevant pathways upon tumor cell and stromal fibroblast interaction. Am J Pathol *179*: 487-501, 2011.
5 Takagi A, Watanabe M, Ishii Y, Morita J, Hirokawa Y, Matsuzaki T and Shiraishi T: Three-dimensional cellular spheroid formation provides human prostate tumor cells with tissue-like features. Anticancer Res *27*: 45-53, 2007.
6 Hirschhaeuser F, Menne H, Dittfeld C, West J, Mueller-Klieser W and Kunz-Schughart LA: Multicellular tumor spheroids: an underestimated tool is catching up again. J Biotechnol *148*: 3-15, 2010.
7 Korkaya H, Paulson A, Iovino F and Wicha MS: HER2 regulates the mammary stem/progenitor cell population driving tumorigenesis and invasion. Oncogene *27*: 6120-6130, 2008.
8 Fujii H, Honoki K, Tsujiuchi T, Kido A, Yoshitani K and Takakura Y: Sphere-forming stem-like cell populations with drug resistance in human sarcoma cell lines. Int J Oncol *34*: 1381-1386, 2009.
9 Gibbs CP, Kukekov VG, Reith JD, Tchigrinova O, Suslov ON, Scott EW, Ghivizzani SC, Ignatova TN and Steindler DA: Stem-like cells in bone sarcomas: implications for tumorigenesis. Neoplasia *7*: 967-976, 2005.
10 Riedl A, Schlederer M, Pudelko K, Stadler M, Walter S, Unterleuthner D, Unger C, Kramer N, Hengstschlager M, Kenner L, Pfeiffer D, Krupitza G and Dolznig H: Comparison of cancer cells in 2D vs 3D culture reveals differences in AKT-mTOR-S6K signaling and drug responses. J Cell Sci *130*: 203-218, 2017.
11 Schroeder A, Mueller O, Stocker S, Salowsky R, Leiber M, Gassmann M, Lightfoot S, Menzel W, Granzow M and Ragg T: The RIN: an RNA integrity number for assigning integrity values to RNA measurements. BMC Mol Biol *7*: 3, 2006.
12 Sato F, Tsuchiya S, Terasawa K and Tsujimoto G: Intra-platform repeatability and inter-platform comparability of microRNA microarray technology. PLoS One *4*: e5540, 2009.
13 Lanczky A, Nagy A, Bottai G, Munkacsy G, Szabo A, Santarpia L and Gyorffy B: miRpower: a web-tool to validate survival-associated miRNAs utilizing expression data from 2178 breast cancer patients. Breast Cancer Res Treat *160*: 439-446, 2016.

14 Huang X, Ding L, Bennewith KL, Tong RT, Welford SM, Ang KK, Story M, Le QT and Giaccia AJ: Hypoxia-inducible mir-210 regulates normoxic gene expression involved in tumor initiation. Mol Cell *35*: 856-867, 2009.
15 Sachdeva M, Zhu S, Wu F, Wu H, Walia V, Kumar S, Elble R, Watabe K and Mo YY: p53 represses c-Myc through induction of the tumor suppressor miR-145. Proc Natl Acad Sci USA *106*: 3207-3212, 2009.
16 Zhang F, Cui J, Liu X, Lv B, Liu X, Xie Z and Yu B: Roles of microRNA-34a targeting SIRT1 in mesenchymal stem cells. Stem Cell Res Ther *6*: 195, 2015.
17 Iwanicki MP, Davidowitz RA, Ng MR, Besser A, Muranen T, Merritt M, Danuser G, Ince TA and Brugge JS: Ovarian cancer spheroids use myosin-generated force to clear the mesothelium. Cancer Discov *1*: 144-157, 2011.
18 Kasagi Y, Harada Y, Morodomi Y, Iwai T, Saito S, Yoshida K, Oki E, Saeki H, Ohgaki K, Sugiyama M, Onimaru M, Maehara Y and Yonemitsu Y: Peritoneal Dissemination Requires an Sp1-Dependent CXCR4/CXCL12 Signaling Axis and Extracellular Matrix-Directed Spheroid Formation. Cancer Res *76*: 347-357, 2016.
19 Chen Y, Chen J, Wang H, Shi J, Wu K, Liu S, Liu Y and Wu J: HCV-induced miR-21 contributes to evasion of host immune system by targeting MyD88 and IRAK1. PLoS Pathog *9*: e1003248, 2013.
20 Miao BP, Zhang RS, Li M, Fu YT, Zhao M, Liu ZG and Yang PC: Nasopharyngeal cancer-derived microRNA-21 promotes immune suppressive B cells. Cell Mol Immunol *12*: 750-756, 2015.
21 Deng Y, Zhao J, Sakurai D, Kaufman KM, Edberg JC, Kimberly RP, Kamen DL, Gilkeson GS, Jacob CO, Scofield RH, Langefeld CD, Kelly JA, Ramsey-Goldman R, Petri MA, Reveille JD, Vila LM, Alarcon GS, Vyse TJ, Pons-Estel BA, Argentine Collaborative G, Freedman BI, Gaffney PM, Sivils KM, James JA, Gregersen PK, Anaya JM, Niewold TB, Merrill JT, Criswell LA, Stevens AM, Boackle SA, Cantor RM, Chen W, Grossman JM, Hahn BH, Harley JB, Alarcomicronn-Riquelme ME, Biolupus, networks G, Brown EE and Tsao BP: MicroRNA-3148 modulates allelic expression of toll-like receptor 7 variant associated with systemic lupus erythematosus. PLoS Genet *9*: e1003336, 2013.
22 Schon MP and Schon M: TLR7 and TLR8 as targets in cancer therapy. Oncogene *27*: 190-199, 2008.
23 Miao R, Wang Y, Wan J, Leng D, Gong J, Li J, Zhang Y, Pang W, Zhai Z and Yang Y: Microarray analysis and detection of MicroRNAs associated with chronic thromboembolic pulmonary hypertension. Biomed Res Int *2017*: 8529796, 2017.
24 Hill KS, Erdogan E, Khoor A, Walsh MP, Leitges M, Murray NR and Fields AP: Protein kinase Calpha suppresses Kras-mediated lung tumor formation through activation of a p38 MAPK-TGFbeta signaling axis. Oncogene *33*: 2134-2144, 2014.

Received August 21, 2018
Revised September 5, 2018
Accepted September 6, 2018